Sensors & Actuators: B. Chemical 376 (2023) 132940

Contents lists available at ScienceDirect

Sensors and Actuators: B. Chemical

journal homepage: www.elsevier.com/locate/snb

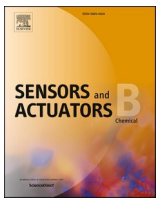

An electrochemical genosensing platform for the relative quantification of the circulating long noncoding RNA CCAT1 to aid in the diagnosis of colorectal cancer

Raquel Sánchez-Salcedo [a,b], Rebeca Miranda-Castro [a,b,*], Noemí de-los-Santos-Álvarez [a,b], Daniel Fernández-Martínez [b,c], Luis Joaquín García-Flórez [b,c,d], María Jesús Lobo-Castañón [a,b,*]

[a] Departamento de Química Física y Analítica, Universidad de Oviedo, Av. Julián Clavería 8, 33006 Oviedo, Spain
[b] Instituto de Investigación Sanitaria del Principado de Asturias, Avenida de Roma, 33011 Oviedo, Spain
[c] Servicio de Cirugía General y del Aparato Digestivo, Hospital Universitario Central de Asturias (HUCA), Avenida de Roma, 33011 Oviedo, Spain
[d] Departamento de Cirugía y Especialidades Médico-Quirúrgicas. Universidad de Oviedo, Av. Julián Clavería 6, 33006 Oviedo, Spain

ARTICLE INFO

Keywords:
Colorectal cancer
Genosensor
Liquid biopsy
Long noncoding RNA

ABSTRACT

Long noncoding RNAs (lncRNAs) are promising biomarkers for the noninvasive diagnosis of colorectal cancer, but detection of cancer-associated changes in their expression levels is now restricted to the use of RT-qPCR. To extend the clinical applicability of these biomarkers, we developed an electrochemical platform, integrated by two different sandwich genosensors, for the relative quantification of a lncRNA called colon cancer associated transcript-1 (CCAT1) with respect to the mRNA GAPDH as an endogenous control. To achieve highly sensitive detection, and in contrast to previous sensors of this class, we use multiple fluorescein-tagged hybridization assistant probes allowing the incorporation of multiple redox enzymes per target molecule, in turn favoring the selective capture of these highly-structured targets onto the sensing platform. The resultant biosensors show high sensitivity (9.7 ± 0.3 μA nM^{-1} for CCAT1 and 7.3 ± 0.1 μA nM^{-1} for GAPDH) and low limits of detection (990 fM and 1830 fM for CCAT1 and GAPDH, respectively). Coupled to a PCR assay, we detect the lncRNA at clinically relevant concentrations. Preliminary results using total RNA extracted from the colorectal cancer cell line HT29 and spiked plasma samples from healthy individuals suggest that this new sensing architecture is sensitive and selective enough to obtain the expression level of CCAT1 simply from the ratio of outputs from the two platform sensors. We envision that the same design could be applied to detect other lncRNAs associated to various malignancies, facilitating early cancer diagnosis.

1. Introduction

Colorectal cancer (CRC), not frequently diagnosed several decades ago, is nowadays the third most common cancer worldwide, accounting for 9.4% of cancer deaths in 2020 [1]. Despite the significant advances in understanding the CRC pathophysiology leading to an increased number of treatment options, survival rate is much higher the earlier the disease is diagnosed [2]. Colonoscopy is the method currently used for early-stage detection of CRC, but it is highly invasive, which causes poor adherence to screening programs [3]. The identification of specific circulating molecular biomarkers, still scarce, is expected to enhance the portfolio of non-invasive CRC screening tests. Within the ongoing search to identify new CRC biomarkers, long non-coding RNAs (lncRNAs) are gaining momentum [4].

LncRNAs constitute a very heterogeneous subset of non-coding transcripts longer than 200 nucleotides in length, which are extensively distributed in the human genome, covering a broad range of molecular and cellular functions [5]. In addition, lncRNAs are expressed in a tissue- and disease-specific manner, with increasing evidences of its crucial role in the progression of different human malignancies [6], including CRC. The abnormal expression of different lncRNAs has been shown to play an important role in the biogenesis, progression, metastasis and invasion or drug resistance in CRC [7].

In this landscape, the lncRNA colon cancer-associated transcript-1 (CCAT1), also termed cancer-associated region long non-coding RNA-5 (CARLo-5), is a 2795-nt RNA transcribed from the chromosome 8q24.21

* Corresponding authors at: Departamento de Química Física y Analítica, Universidad de Oviedo, Av. Julián Clavería 8, 33006 Oviedo, Spain
E-mail addresses: mirandarebeca@uniovi.es (R. Miranda-Castro), mjlc@uniovi.es (M.J. Lobo-Castañón).

https://doi.org/10.1016/j.snb.2022.132940
Received 12 September 2022; Received in revised form 28 October 2022; Accepted 31 October 2022
Available online 2 November 2022

(RefSeq NR_108049.1). In 2012, it was first reported that the expression levels of CCAT1 in colon adenocarcinoma tissues were significantly higher than in the normal colon mucosa, [8] which was more recently confirmed by genome-wide association analysis [9]. In addition, this up-regulation occurs through the different disease stages, from pre-malignant lesions to advanced metastatic conditions [10]. The levels of CCAT1 in plasma were also found higher in CRC patients than in healthy individuals [11]. This opens the possibility of developing liquid biopsy tests based on the detection of CCAT1 for a minimally invasive screening or diagnosis of CRC.

Current knowledge of CCTA1 expression levels in both tissue and plasma samples is mainly based on quantitative reverse transcription polymerase chain reaction (RT-qPCR) measurements [8–14]. Although this is the gold standard for nucleic acid quantification, there is a need for new technologies supporting the accurate and rapid detection of this type of biomarkers in biological fluids, which allow their implementation in general clinical or biochemical laboratories and not only in core facilities [15,16]. The utility of hybridization-based assays in nucleic acid detection suggests that this technology would also be useful for the detection of lncRNAs. However, only one molecular assay has been described so far, in which the specific hybridization of the target RNA to a peptide nucleic acid-based molecular beacon is used to detect CCAT1 directly in tissue samples [17,18].

Detection of cancer-related lncRNAs requires highly sensitive approaches, and some recent efforts have focused on the use of functional nanomaterials that allow signal amplification after target recognition by the affinity interaction. In this way, several genosensors have been reported for detecting lncRNAs related to different types of cancer as MALAT1 (non-small cell lung cancer) [19] or HULC (liver cancer) [20,21]. Alternatively, target preconcentration based on magnetic beads [22] has been applied to the measurement of HOTAIR, a lncRNA up-regulated in ovarian cancer among others. However, while these approaches provide limits of detection in the low femtomolar range for the detection of synthetic targets, their application to biological samples is more challenging. Detectability can be further improved if the genosensor is coupled to an isothermal nucleic acid amplification such as recombinase polymerase amplification (RPA) [23] or loop-mediated isothermal amplification (LAMP) [24]. But from a clinical point of view and to avoid misinterpretation of results, it is very important to perform a relative quantification using an endogenous control (also known as reference or housekeeping gen) for normalization, which has only been done so far in two previous works [24,25].

The development of highly sensitive genosensors for lncRNA detection is also hampered by the stable and strong secondary structure of these targets that must be disrupted for their specific recognition by the capture probe (CP) in the sensing phase. To overcome this, we have designed a new sensing strategy that exploits the great length of these targets to incorporate multiple detection probes (DPs) in a sandwich format [25]. This allows to disrupt the secondary structure of the lncRNA and, in turn, produces an amplified measurable electrochemical readout. Expanding on this, here we describe the design and characterization of two genosensors for the detection of CCAT1 and the mRNA glyceraldehyde-3-phosphate dehydrogenase (GAPDH) as endogenous control. The sensors are challenged with the product of a customized PCR for simultaneously amplifying the two targeted sequences. To the best of our knowledge, this is the first electrochemical platform that is able to perform the relative quantification of CCAT1 in plasma samples by comparing the readout of both sensors.

2. Experimental section

2.1. Apparatus and reagents

Synthetic oligonucleotides were purchased as lyophilized powder with HPLC-purification grade from Metabion (Germany) and are listed in Table S1. *p*-Aminothiophenol, concentrated saline sodium phosphate-EDTA 20 × concentrate (20 × SSPE), phosphate buffered saline 10 × concentrate (10 × PBS), bovine serum albumin (BSA) and 3,3′,5,5′ tetramethylbenzidine (TMB) substrate for peroxidase including H_2O_2, were obtained from Sigma-Aldrich (Spain). Anti-fluorescein-peroxidase Fab fragment (antiF-POD) was purchased from Roche diagnostics (Spain). 1% casein blocking in 1 × PBS was supplied by Thermo Scientific (Spain). Aqueous solutions were prepared with ultrapure and RNAse/DNAse free water (resistivity: 18.2 MΩ.cm) obtained from a Milli-Q System with a Biopak Polisher ultrafiltration cartridge (Millipore). EZNA Total RNA Kit I and mRNeasy Serum/Plasma advanced kit were acquired from Omega Bio-tek (USA) and from Qiagen, respectively.

All the measurements were performed with an Autolab PGSTAT 12 controlled by the software Nova 2.1.4 (Eco-chemie, The Netherlands). The genosensors were built onto the gold working electrode (Ø 4 mm) of a 3-electrode screen-printed cell (DRP-220BT) provided by Metrohm-DropSens (Asturias-Spain). The cell also incorporates a gold auxiliary electrode and a silver pseudo-reference electrode.

2.2. Construction of genosensors

Prior to sensor fabrication, the screen-printed electrodes (SPAuE) were rinsed with ethanol and water and dried under a stream of nitrogen. Then, 40 μL of a 0.5 M H_2SO_4 solution were placed onto the cell, which was subjected to an electrochemical treatment that consisted of 10 potential cycles between 0 and 1.3 V at 100 mV/s, until a stable cyclic voltammogram was obtained. Finally, the electrodes were rinsed with deionized water and dried under nitrogen stream just before the formation of the sensing surface.

Binary self-assembled monolayers (SAMs) were prepared by first incubating overnight the clean gold electrodes in a 1 μM solution of the thiolated capture probe in 2 × SSPE buffer pH 7 at 4 °C under a water-saturated atmosphere. Subsequently, the electrodes were washed with 2 × SSPE and incubated for 50 min in a 1 mM *p*-aminothiophenol solution in 2 × SSPE at room temperature (RT) to block the bare gold surface. Unbound thiols were then removed by thoroughly washing with 2 × SSPE buffer.

2.3. Genosensors operation

The sensors for the specific recognition of lncRNA CCAT1 and the endogenous control GAPDH operate with a sandwich-hybridization format, which occurs in two consecutive steps. First, a 200 nM solution of the DPs was incubated with increasing concentrations of the target in 2 × SSPE at 95 °C for 5 min (a 3-minute time period at 70 °C for the RNA samples to maintain their integrity) and immediately cooled in ice. After bringing to RT, the same volume of a 5% BSA solution was added to this solution giving a final concentration of 100 nM DPs and 2.5% BSA. An aliquot of 10 μL of the preformed hybrid was then placed onto the genosensor surface and incubated for 2 h at RT (protected from light), where the heterogeneous hybridization takes place. The electrodes were washed with 2 × SSPE and incubated with a solution of 1% casein blocking buffer in 1 × PBS for 10 min, followed by the enzyme labeling with 0.5 U/mL of antiF-POD conjugate in casein blocking buffer for 30 min in darkness. Immediately after, the SPAuE was washed with 2 × SSPE and dried. Then, it was covered by 40 μL of the enzymatic substrate solution (TMB + H_2O_2), and the enzymatic reaction proceeded for 60 s, after which, the current due to the electrochemical reduction of the enzymatically oxidized TMB was measured by chronoamperometry at 0 V for 60 s. The incubation stages were performed at RT unless otherwise indicated and volumes of 10 μL were used to cover the working electrodes in all stages.

2.4. RNA extraction from HT29 cells

RNA from thawed HT29 cell pellets from the American Type Culture

Collection (ATCC) (culture conditions are specified in the Supporting Information) was extracted by using the EZNA Total RNA Kit I (Omega Bio-tek, USA) following the manufacturer's protocol. Briefly, the extraction consists of the lysis of the cells employing a guanidinium thiocyanate buffer, transfer of the homogenized lysate to silica spin columns followed by serial washing steps with the recommended buffers and, finally, RNA elution by RNase-free water (50 μL) preheated at 70 °C by centrifugation at maximum speed (16,000 *g*). The concentration of the total RNA extracted was determined by a Qubit fluorometer RNA quantification assay. The RNA solutions were stored at − 80 °C until further analysis.

2.5. Plasma collection

Blood samples from healthy donors were collected in EDTA-containing tubes by venipuncture at the Hospital Universitario Central de Asturias. The samples were kept at 4 °C until processing, which was carried out ideally within 30 min after collection and never after one hour had elapsed. Plasma separation was accomplished by centrifugation at 1500 *g* for 15 min at 4 °C. The upper phase was carefully transferred to a new tube and it was centrifuged at 3000 *g* for 15 min at 4 °C. Subsequently, the plasma was aliquoted and stored at − 80 °C until RNA extraction. The study was approved by the ethical committee of Principado de Asturias.

2.6. RNA extraction from plasma samples

RNA extraction from plasma samples was carried out with the mRNeasy Serum/Plasma advanced kit from Qiagen following the manufacturer's protocol employing 200 μL of plasma. This protocol consisted of guanidine-based lysis of the sample, followed by precipitation of some inhibitors (mostly proteins) and purification on silica-membrane columns with consecutive washing stages using the buffers supplied with the kit. The RNA was eluted in 20 μL of RNase-free water.

2.7. RT-qPCR and end point RT-PCR

Reverse transcription quantitative PCR (RT-qPCR) was run in a 7900HT Fast Real-Time PCR System (Thermo Fisher Scientific), using PrimeTime One-step RT-qPCR Master Mix (IDT) that allows both enzymatic reactions, reverse transcription and PCR amplification, to be carried out in a single tube. This is a ready-to-use master mix including all components for RNA amplification and detection except primers and template (i.e. antibody-mediated hot-start DNA polymerase, reverse transcriptase, dNTPs, $MgCl_2$, enhancers, and stabilizers are present). Reference dye is also provided but not included in the master mix. Likewise, TaqMan Gene Expression Assays including target primers and a sequence-specific TaqMan MGB® probe labeled with FAM were used for CCAT1 (Hs04402620_m1) and GAPDH (Hs00266705_g1). The PCR reactions were performed in a volume of 10 μL containing 10 ng of total RNA extracted from HT29 cells. The cycling program included reverse transcription for 15 min at 50 ºC, polymerase activation at 95 ºC for 3 min, followed by 40 cycles of denaturation at 95 ºC for 3 min, annealing and extension at 50 ºC for 30 s. Each reaction was carried out in duplicate. C_t values were calculated with the integrated SDS 2.4 software.

The end-point RT-PCR was also performed by using PrimeTime One-step RT-qPCR Master Mix (IDT), without the addition of the reference dye, in a final volume of 10 μL. The primers were specifically designed for each gene flanking the sequence recognized by the corresponding biosensor (Table S1). The amplification conditions were: 15 min at 50 ºC and 30 s at 94 ºC for cDNA synthesis and polymerase activation, respectively, followed by PCR amplification in 28 cycles of 94 ºC for 30 s for denaturation, 55 ºC for 30 s for annealing, 72 ºC for 60 s for extension. Reactions were conducted in a GeneAmp® PCR System 2700 thermocycler (Thermo Fisher Scientific). Afterward, the concentration of the generated amplicons was estimated by fluorescence with a Qubit dsDNA Broad Range quantification assay kit (Thermo Fisher Scientific).

3. Results and discussion

3.1. Design of genosensors for CCAT1 and GAPDH

Sandwich hybridization-based sensors have proven to be of significant utility for the detection of DNA and RNA sequences. However, to apply this technology to the development of minimally invasive tests based on the detection of the lncRNA CCAT1, which may be useful in CRC diagnosis, it is necessary to take into account some considerations. First, the assay must accurately determine the lncRNA at very low levels in a complex sample such as serum or plasma. The length of the target and its strong secondary structure are crucial factors that must be considered to minimize loss of sensitivity. In addition, RNA must be extracted from the sample, and a relative quantification is needed to reduce errors due to variations in the quality and quantity of the extracted RNA. This involves determining the changes in CCAT1 expression relative to the levels of an internal control RNA, which is stably expressed in the investigated samples.

To surmount these difficulties, we have developed two sensors for the detection of specific fragments of CCAT1 and GAPDH, which is a common endogenous reference gene. The design is based on a general strategy that we have previously described to maximize the sensitivity of the sandwich-type genosensors [25]. By selecting a target sequence of sufficient length, it is possible to design various detection probes (DPs), which simultaneously hybridize with the complementary regions of the target. In this way, once the duplex is entrapped onto the sensing phase, a single target will bind multiple redox enzymes used as reporter molecules, with the subsequent signal amplification.

A critical step in the design is the *in silico* selection of the targeted sequence and the concomitant complementary probes because the set of selected oligonucleotides will determine both the sensitivity and selectivity of the sensing platform. The transcript sequences corresponding to CCAT1 (NR_108049.1) and GAPDH (NM_001289746.2) were obtained from the Genbank database [26]. First, we checked the secondary structures of the transcripts using the RNAfold algorithm in the RNA-Vienna package (Fig. S1) [27]. As expected, both have a strong secondary structure, and the first criteria we adopted for selecting an appropriate region of these transcripts as the target is to minimize the self-structures like stem-loops and hairpins. The targeted regions in RT-qPCR approaches previously developed are a good starting point. In the case of GAPDH, the most frequently amplified regions are in the first exon, while for CCAT1, all previous RT-qPCR methods targeted sequences located in the region where exon 1 ends and exon 2 starts. The length of the target is another important issue. It is kept in the range between 65 nt and 200 nt, long enough to allow the design of multiple DPs and short enough to make possible the formation of a full dsDNA on the surface after hybridization with CP and DPs. Primer Blast, a tool for designing specific primers for PCR assays [28], was used to identify unique sequences in each gen, within this size range, that could serve as target sites. The returned list of potential targets was analyzed in terms of the stability of their secondary structure using the Mfold tool [29], selecting that with the less stable one.

The 88nt fragment (between 2449 and 2536 positions) of CCAT1 and the 75nt (from 315 to 389 positions) for GAPDH meet the above criteria and were selected as targets for the genosensors design. The secondary structure of these fragments, as predicted using the Mfold algorithm [29], is shown in Fig. 1A. A CP, complementary to the 3′ end of the target, and various DPs, complementary to the rest of the sequence, were designed to disrupt its hairpin structures, ensuring the formation of a continuous duplex after recognition, with the subsequent improved sensitivity (Fig. 1A and Table S1) [30].

The sensing phase is constructed by immobilizing the designed CP on gold electrodes (Fig. 1B). In a first operational step, the homogeneous

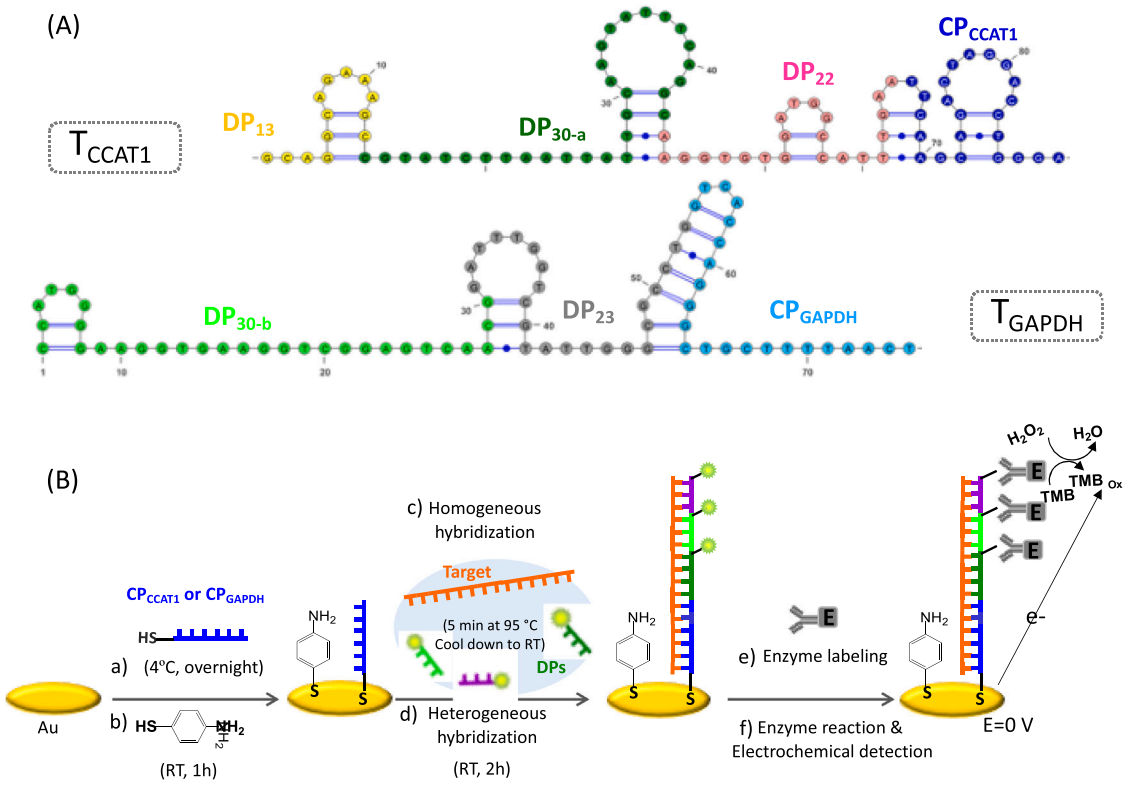

Fig. 1. (A) Most stable secondary structures of T_{CCAT1} (88-mer specific sequence of CCAT1) and T_{GAPDH} (75-mer specific sequence of GAPDH) at 25 °C and 0.3 M Na^+ from Mfold software and drawn with VARNA applet (https://varna.lri.fr/). Colored regions are complementary to the indicated capture probe (CP) or detection probes (DPs). (B) Genosensor design.

hybridization between fluorescein-labeled DPs and the target in solution contributes to its unwinding, and improves the efficiency of the hybridization with the electrode-bound CP. After the recognition step, the multiple 6-FAM tags are bound to the antiF-POD enzyme conjugate, which catalyzes the oxidation of the redox-active substrate 3,3′,5,5′-tetramethylbenzidine (TMB). The final readout is obtained by chronoamperometry.

3.2. Methodology optimization and performance assessment

The first step in the fabrication of the sensors is the selection of an appropriate method for immobilizing the CP on the electrode surface. Many of the genosensors built on gold surfaces use for this purpose a mixed SAM of a thiol-CP and 6-mercaptohexanol as a blocker [30]. However, this approach has been shown to lead to a heterogeneous distribution of the CP on the surface and an incomplete blocking of the bare gold, leading to relatively high background signals and low hybridization efficiency, which compromise sensitivity. Because the use of SAMs of aromatic thiols for the immobilization of CP has been shown to provide lower background signals, while increasing the electron transfer through the sensing layer [31], we explored two immobilization methods for improving sensitivity: i) the chemisorption of the thiolated-CP, using *p*-aminothiophenol as a blocker and ii) covalent binding of the amine-CP to a pure monolayer of *p*-mercaptobenzoic acid.

We challenged the sensors prepared for the set of oligonucleotides specific for CCAT1 by both methods to increasing amounts of a DNA analog of the target RNA to minimize issues related to RNA instability. In the absence of the target, both methods gave comparable and very low

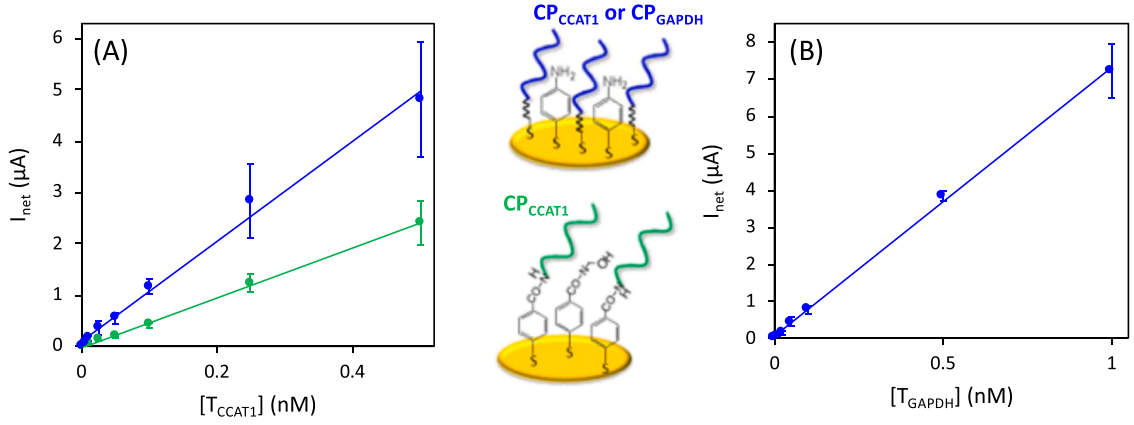

Fig. 2. Calibration plots for the determination of the synthetic targets T_{CCAT1} (A) and T_{GAPDH} (B), when using a mixed SAM approach (blue) or a pure SAM approach (green).

background signals [(12 ± 3) nA and (14 ± 5) nA with mixed and pure SAM approaches, respectively]. In the presence of target DNA, the mixed SAM approach produced a larger increase in the signal (Fig. 2), leading to an improved detection limit. Thus, with this immobilization method we achieved a detection limit of 990 fM (obtained as three times the standard deviation of the blank divided by the slope), above which we obtained a linear increase of the signal with increasing target concentrations in the range of 5–500 pM (I_{net} (μA) = (9.7 ± 0.4) [CCAT1] (nM) + (0.10 ± 0.07); r = 0.996). A reproducibility of 21% was achieved over the whole linear range. In contrast, we obtained a 1.8 pM detection limit within the same linear range (I_{net} (μA) = 4.85 ± 0.07) [CCAT1] (nM) - (0.02 ± 0.02); r = 0.9995) using the sensor prepared by covalent immobilization of the CP on a pure SAM, half that of the mixed-SAM method. The operation parameters such as incubation times, concentration of detecting probes and POD conjugate were fixed according to previous studies [25].

Based on these results and on the ease of its fabrication we employed the mixed-SAM approach including *p*-aminothiophenol for developing the genosensor targeting the 75 nt fragment of GAPDH mRNA for normalization purposes (Fig. 1). In this case, the target sequence hybridizes with two fluorescein-labeled detection probes designed with an equivalent procedure to that used for the target transcript. This sensor detects its target DNA with a linear range from 10 pM to 1 nM (I_{net} (μA) = (7.3 ± 0.1) [GAPDH] (nM) + (0.04 ± 0.05); r = 0.9995), an average RSD of 18.5% and a detection limit of 1.83 pM (Fig. 2).

Comparing the analytical performance of both genosensors, we observe that the sensitivity for CCAT1 is 1.34 times larger than that of the GAPDH sensor. This stems from the use of three detection probes in the CCAT1 design instead of the two used for the measurement of the endogenous control, which affords the incorporation of theoretically 1.5 times more redox enzyme molecules per hybridization event, with the consequent increase in the signal. These results support the possibility of tuning the sensitivity of the assay by controlling the number of DP to match the expression level of the corresponding target in the sample.

3.3. Monitoring of CCAT1 in tumor cell lines

We next applied the genosensors to the detection of the targeted RNAs extracted from the tumor cell line HT29, which corresponds to a human colorectal adenocarcinoma tissue. First, the relative abundance of CCAT1 with respect to GAPDH in the extracted total RNA was estimated by RT-qPCR using a specific primer for the reverse transcription and a Taqman assay for the subsequent amplification of the cDNA. The primers used for the amplification of cDNA cross an exon-exon junction. In this way, the intron in the DNA sequence would not be amplified, avoiding interference from contaminating genomic DNA. Amplification efficiencies of CCAT1 and GAPDH amplicons were determined using serial dilutions of total RNA. The number of cycles (C_t) needed to produce the same defined threshold fluorescence depends linearly on the amount of RNA (Fig. S2), and from the slope of the corresponding plots we obtained an amplification factor ($E = 10^{(-1/slope)}$) of 1.935 and 1.910 for CCAT1 and GAPDH, respectively, which corresponds to amplification efficiencies: ($10^{(-1/slope)}$-1) × 100 of 93.5% and 91%.

In qPCR the number of target molecules producing the threshold fluorescence N_{Ct} is given by: $N_{Ct} = N_0 E^{Ct}$, where N_0 is the initial number of target molecules; in consequence, assuming that the number of CCAT1 and GAPDH amplicons at C_t are equivalent [32], the relative amount of CCAT1 in the extracted RNA, expressed as the ratio between the initial number of the target and reference molecules (*r*) is given by [33]:

$$r = \frac{N_{0,CCAT1}}{N_{0,GAPDH}} = \frac{N_{Ct,CCAT1}\, E_{CCAT1}^{-Ct,CCAT1}}{N_{Ct,GAPDH}\, E_{GAPDH}^{-Ct,GAPDH}} \approx \frac{E_{CCAT1}^{-Ct,CCAT1}}{E_{GAPDH}^{-Ct,GAPDH}}$$

From the qPCR data (Table S2), we thus estimated that the amount of CCAT1 transcript in the HT29 cells is 0.040 ± 0.001 times the reference GAPDH gene. This result underlines the need for a more sensitive method for the detection of CCAT1 than GAPDH, which, in the present work, is addressed using a different number of detection probes and, consequently, a different number of enzymatic markers per target molecule.

The CCAT1 genosensor responded conveniently when challenged with total RNA extracted from HT29 cell pellets containing between 2×10^6 and 5×10^6 cells. Signals ranging from 47 to 141 nA, clearly distinguishable from those recorded for the calibration blank, were obtained. Moreover, we observed a signal increase upon the addition to the extracts of 5 and 10 pM of the synthetic DNA target, from which we estimated an amount of CCAT1 in HT29 cells of approximately 0.02 ± 0.01 ng / μg total RNA (see supporting information). The selectivity of the sensor is also reasonable. We used as a negative control total RNA extracted from about 2 million LNCaP cells, which were isolated from human prostate adenocarcinoma tissue and do not express CCAT1 [34]. The measured current intensity was (25 ± 11) nA, not significantly higher than the signal corresponding to the calibration blank (Fig. S3). This result was confirmed by RT-qPCR (Fig. S4) from which it is apparent that RNA extracts from LNCaP cells express GAPDH but not CCAT1. Taken together, the CCAT1 biosensor would allow direct detection of the lncRNA CCAT1 present in several millions of HT29 cells. However, quantification for liquid biopsy test is compromised to some extent since the levels of circulating lncRNAs in plasma might be lower than in cell lines.

Bearing in mind the sensitivity constraints, it was decided to couple the developed genosensors to a previous RT-PCR amplification stage. With this aim, the RNA extracted from the tumor cells was 10-fold diluted from 100 ng to 0.01 ng and subjected to end-point RT-PCR as described above in the protocols section. The amplicons obtained in the PCR for both CCAT1 and the endogenous control were detected with the corresponding sensor.

To guarantee a reliable quantification of CCAT1 and GAPDH copies and, in turn, the relationship between the starting amount of transcript and the electrochemical signal obtained for the PCR products, the amplification should be conducted up to its exponential stage, avoiding the plateau stage when reaction components become limited. On the basis of the RT-qPCR amplification curves shown in Fig. S4, and trying to detect the lowest amount of lncRNA possible, we selected 30 and 27 cycles of amplification for CCAT1 and GAPDH, respectively. The results in Fig. 3 display the capability of the combination of RT-PCR amplification and the electrochemical sequence-specific biosensors to individually quantify CCAT1 and GAPDH in the tumor cell line HT29. The electrochemical signals recorded with both genosensors increase

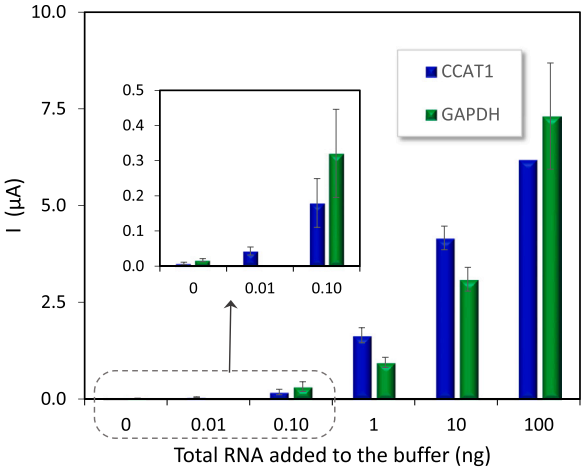

Fig. 3. Response of the CCAT1 (blue) and GAPDH (green) sensors to the RT-PCR amplification products obtained after 30 (CCAT1) or 27 (GAPDH) cycles, starting from different amounts of total RNA extracted from HT29 cells.

monotonically with increasing amount of starting total RNA from HT29 until they approach saturation. However, as the number of amplification cycles for the target and housekeeping gene is different, the relative amount of CCAT1 to GAPDH is not conserved after amplification.

3.4. Detection of CCAT1 in plasma samples

Having established that we could detect lncRNA in the HT29 cells and taking into account the lack of standards for the selected transcript, we next analyzed plasma samples from healthy individuals that were fortified with 10 ng of RNA extracted from the tumor cells. The efficiency of plasma extraction was verified by means of RT-qPCR, comparing the difference in C_t obtained for both genes ($\Delta Ct = C_{t,\ CCAT1} - C_{t,\ GAPDH}$) in buffer and in different plasmas. No significant differences in ΔCt were observed (Table S3), suggesting that the method used for the extraction of RNA from plasma samples is highly effective.

To avoid the need for two independent amplifications, one for each transcript, we performed 28 cycles of end-point RT-PCR after the extraction of RNA from plasma samples spiked with serial dilutions, from 5 ng to 0.01 ng, of total RNA from HT29 cells. Subsequently, the CCAT1 and GAPDH genosensors were challenged with the corresponding amplicons after a dilution 1:100. The net signal, subtracting that obtained for the plasma, increased with the initial amount of total RNA added, until approaching saturation (Fig. 4A). The resultant response curves were fitted to the Langmuir model:

$$I = \frac{I_{max}\, m_{total\ RNA}(ng)}{K + m_{total\ RNA}(ng)}$$

by using Origin software, obtaining the following equations:

$$For\ \ CCAT1 : I_{net}(\mu A) = \frac{1.92(\pm 0.17)\cdot m_{total\ RNA}(ng)}{2.31(\pm 0.51) + m_{total\ RNA}(ng)};\ R^2 = 0.993$$

$$For\ GAPDH : I_{net}(\mu A) = \frac{2.29(\pm 0.32)\cdot m_{total\ RNA}(ng)}{0.11(\pm 0.08) + m_{total\ RNA}(ng)};\ R^2 = 0.994$$

The saturation signal was 1.2 times larger for the housekeeping transcript, which may stem from the shorter length of the duplex on surface after hybridization. In the linear region of the response curve, in contrast, the slope (I_{max}/K) is 25 times higher for GAPDH, in agreement with the higher expression level of GAPDH than CCAT1 in the cells. This leads to a relative amount of CCAT1 transcript to GAPDH in the HT29 cells $r = 0.04$, similar to that obtained by RT-qPCR. Therefore, using the ratio of signal of both sensors, provided the measurements are performed in the linear range, it is possible to estimate the relative expression of the target transcript in relation to the reference one.

Finally, to illustrate the usefulness of a dual electrochemical platform integrating both sensors, we performed the RT-PCR amplification (28 cycles) of the two targets, simultaneously in a single reaction. The performance of the genosensors in the multiplexed amplicons is not significantly different from that observed on the separate amplification products (Fig. 4). These data highlight the promise of the proposed electrochemical sensors for the relative quantification of the CCAT1 expression levels in plasma samples.

4. Conclusions

In this study, we present an electrochemical platform for the relative quantification of lncRNAs, which is integrated by two genosensors for detecting a specific transcript and a housekeeping sequence. It is used in the analysis of the lncRNA CCAT1, a biomarker specific of colorectal cancer, in plasma samples spiked with total RNA extracted from a tumor cell line. Its key features include high sensitivity and specificity. Coupled to end-point RT-PCR, the ratio between the signals of target and reference transcripts in a single sample can be used to calculate the relative gene expression level. Although we focused on CCAT1, our method

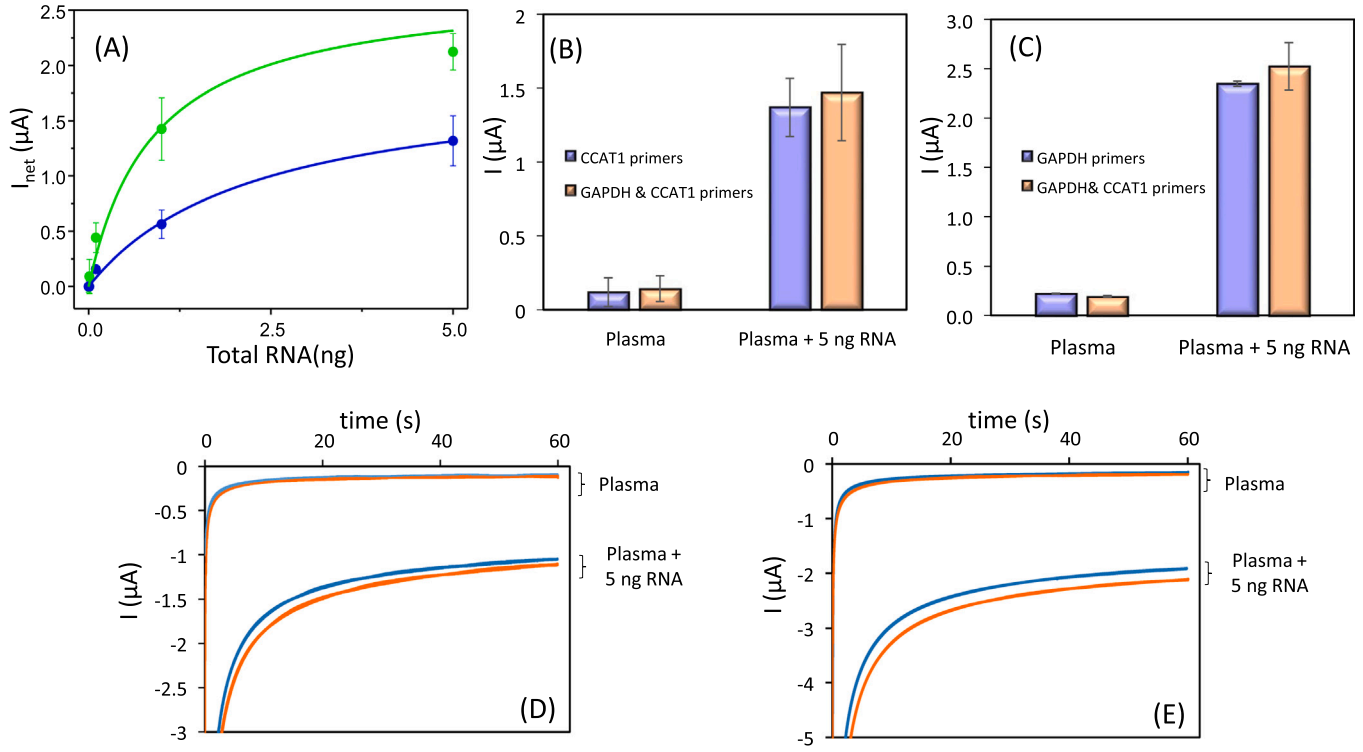

Fig. 4. (A) Signals recorded with CCAT1 (blue) and GAPDH (green) genosensors after previous and independent end-point RT-PCR amplification (28 cycles) of plasma samples supplemented with different amounts of RNA. The data are fitted to the Langmuir model. (B) Signals obtained with the CCAT1 sensor and (C) with the GAPDH sensor, when coupled to the individual (blue) or simultaneous (orange) RT-PCR amplification (28 cycles) of both transcripts. The corresponding chronoamperograms recorded with the CCAT1 (D) and the GAPDH (E) genosensor are shown as well.

could be applied to other lncRNA associated to different malignancies for which an altered expression level has been described.

CRediT authorship contribution statement

Raquel Sánchez Salcedo: Methodology, Investigation, Data curation, Writing – original draft, Writing – review & editing. **Rebeca Miranda-Castro**: Conceptualization, Supervision, Data curation, Methodology, Writing – review & editing. **Noemí de-los-Santos Álvarez**: Conceptualization, Supervision, Data curation, Methodology, Writing – review & editing. **Daniel Fernández-Martínez**: Conceptualization, Writing – review & editing. **Luis Joaquín García-Flórez**: Conceptualization, Writing – review & editing. **María Jesús Lobo-Castañón**: Conceptualization, Resources, Project administration, Supervision, Writing – review & editing.

Declaration of Competing Interest

The authors declare that they have no known competing financial interests or personal relationships that could have appeared to influence the work reported in this paper.

Data availability

The authors confirm that the data supporting the results of this study are available within the article and its supplementary material.

Acknowledgment

This research was funded by the Spanish Government (project RTI-2018–095756-B-I00). R.S.S. thanks the Spanish Government for a PhD fellowship (MCIU-20-PRE2019–087618).

Supplementary data

Additional experimental protocols and calculations, supplementary Tables and Figures, as indicated in the text (PDF), can be found on line.

Appendix A. Supporting information

Supplementary data associated with this article can be found in the online version at doi:10.1016/j.snb.2022.132940.

References

[1] Y. Xi, Y. P. Xu, Global colorectal cancer burden in 2020 and projections to 2040, Transl. Oncol. 14 (2021), 101174.
[2] E. Dekker, P.J. Tanis, J.L.A. Vleugels, P.M. Kasi, M.B. Wallace, Colorectal cancer, Lancet 394 (2019) 1467–1480.
[3] J.M. Inadomi, Screening for colorectal neoplasia, N. Engl. J. Med 376 (2017) 149–156.
[4] Y. Yang, X. Yan, X. Li, Y. Ma, A. Goel, Long non-coding RNAs in colorectal cancer: novel oncogenic mechanisms and promising clinical applications, Cancer Lett. 504 (2021) 67–80.
[5] J.J. Quinn, H.Y. Chang, Unique features of lncRNA biogenesis and function, Nat. Rev. Genet. 17 (2016) 47–62.
[6] T. Gutschner, S. Diederichs, The hallmarks of cancer: a long non-coding RNA point of view, RNA Biol. 9 (2012) 703–719.
[7] S. Chen, X. Shen, Long noncoding RNAs: functions and mechanisms in colon cancer, Mol. Cancer 19 (2020) 167.
[8] A. Nissan, A. Stojadinovic, S. Mitrani-Rosenbaum, D. Halle, R. Grinbaum, M. Roistacher, A. Bochem, B.E. Dayanc, G. Ritter, I. Gomceli, E.B. Bostanci, M. Akoglu, Y.T. Chen, et al., Colon cancer associated transcript-1: a novel RNA expressed in malignant and pre-malignant human tissues, Int. J. Cancer 130 (2012) 1598–1606.
[9] F. Jing, H. Jin, Y. Mao, Y. Li, Y. Ding, C. Fan, K. Chen, Genome-wide analysis of long non-coding RNA expression and function in colorectal cancer, Tumour Biol. 39 (2017), 1010428317703650.
[10] B. Alaiyan, N. Ilyayev, A. Stojadinovic, et al., Differential expression of colon cancer associated transcript1 (CCAT1) along the colonic adenoma-carcinoma sequence, BMC Cancer 13 (2013) 196.
[11] W. Zhao, M. Song, J. Zhang, M. Kuerban, H. Wang, Combined identification of long non-coding RNA CCAT1 and HOTAIR in serum as an effective screening for colorectal carcinoma, Int. J. Clin. Exp. Pathol. 8 (2015) 14131–14140.
[12] T. Ozawa, T. Matsuyama, Y. Toiyama, N. Takahashi, T. Ishikawa, H. Uetake, Y. Yamada, M. Kusunoki, G. Calin, A. Goel, CCAT1 and CCAT2 long noncoding RNAs, located within the 8q.24.21 'gene desert', serve as important prognostic biomarkers in colorectal cancer, Ann. Oncol. 28 (2017) 1882–1888.
[13] E. Gharib, E. Nazemalhosseini-Mojarad, K. Baghdar, Z. Nayeri, H. Sadeghi, S. Rezasoltani, A. Jamshidi-Fard, P. Larki, A. Sadeghi, M. Hashemi, H.A. Aghdaei, Identification of a stool long non-coding RNAs panel as a potential biomarker for early detection of colorectal cancer, J. Clin. Lab. Anal. 35 (2021), e23601.
[14] T. Takeda, Y. Yokoyama, H. Takahashi, D. Okuzaki, K. Asai, H. Itakura, N. Miyoshi, S. Kobayashi, M. Uemura, T. Fujita, H. Ueno, M. Mori, Y. Doki, H. Fujii, H. Eguchi, H. Yamamoto, A stem cell marker KLF5 regulates CCAT1 via three-dimensional genome structure in colorectal cancer cells, Br. J. Cancer 126 (2022) 109–119.
[15] R. Miranda-Castro, N. de-los-Santos-Álvarez, M.J. Lobo-Castañón, Long noncoding RNAs: from genomic junk to rising stars in the early detection of cancer, Anal. Bioanal. Chem. 411 (2019) 4265–4275.
[16] Y.-M. Wang, M.P. Trinh, Y. Zheng, K. Guo, L.A. Jimenez, W. Zhong, Analysis of circulating non-coding RNAs in a non-invasive and cost-effective manner, Trends Anal. Chem. 117 (2019) 242–262.
[17] Y. Kama, A. Rubinstein, S. Naik, I. Djavsarov, D. Halle, I. Ariel, A.O. Gure, A. Stojadinovic, H. Pan, V. Tsivin, A. Nissan, E. Yavin, Detection of a long non-coding RNA (CCAT1) in living cells and human adenocarcinoma of colon tissues using FIT–PNA molecular beacons, Cancer Lett. 352 (2014) 90–96.
[18] D. Hashoul, R. Shapira, M. Falchenko, O. Teppera, V. Paviovb, A. Nissanb, E. Yavin, Red-emitting FIT-PNAs: "On site" detection of RNA biomarkers in fresh human cancer tissues, Biosens. Bioelectron. 137 (2019) 271–278.
[19] M. Chen, D. Wu, S. Tu, C. Yang, D. Chen, Y. Xu, A novel biosensor for the ultrasensitive detection of the lncRNA biomarker MALAT1 in non-small cell lung cancer, Sci. Rep. 11 (2021) 3666.
[20] F. Liu, G. Xiang, D. Jiang, L. Zhang, X. Chen, L. Liu, F. Luo, Y. Li, C. Liu, X. Pu, Ultrasensitive strategy based on PtPd nanodendrite/nano-flower-like@GO signal amplification for the detection of long non-coding RNA, Biosens. Bioelectron. 74 (2015) 214–221.
[21] J.-J. Lia, L. Shang, L.-P. Jia, R.-N. Ma, W. Zhang, W.-L. Jia, H.-S. Wang, K.-H. Xu, An ultrasensitive electrochemiluminescence sensor for the detection of HULC based on Au@Ag/GQDs as a signal indicator, J. Electroanal. Chem. 824 (2018) 114–120.
[22] N. Soda, M. Umer, S. Kasetsirikul, C. Salomon, R. Kline, N.-T. Nguyen, B.H. A. Rehm, M.J.A. Shiddiky, An amplification-free method for the detection of HOTAIR long noncoding RNA, Anal. Chim. Acta 1132 (2020) 66–73.
[23] M.N. Islam, S. Moriam, M. Umer, H.-P. Phan, C. Salomon, R. Kline, N.-T. Nguyen, M.J.A. Shiddiky, Naked-eye and electrochemical detection of isothermally amplified HOTAIR long non-coding RNA, Analyst 143 (2018) 3021.
[24] L. Moranova, M. Stanik, R. Hrstka, S. Campuzano, M. Bartosik, Electrochemical LAMP-based assay for detection of RNA biomarkers in prostate cancer, Talanta 238 (2022), 123064.
[25] R. Sánchez-Salcedo, R. Miranda-Castro, N. de-los-Santos-Álvarez, M.J. Lobo-Castañón, Dual electrochemical genosensor for early diagnosis of prostate cancer through lncRNAs detection, Biosens. Bioelectron. 192 (2021), 113520.
[26] GenBank database ⟨https://www.ncbi.nlm.nih.gov/genbank⟩, last accessed September 6, 2022.
[27] R. Lorenz, S.H. Bernhart, C.H. Siederdissen, H. Tafer, C. Flamm, P.F. Stadler, I. L. Hofacker, Vienna Package 2. 0 Algorithms Mol. Biol. 6 (2011) 26. ⟨http://www.tbi.univie.ac.at/RNA⟩. last accessed September 6, 2022.
[28] J. Ye, G. Coulouris, I. Zaretskaya, I. Cutcutache, S. Rozen, T.L. Madden, Primer-blast a tool to design target-specific primers for polymerase chain reaction, BMC Bioinform 13 (2012) 134. ⟨http://www.ncbi.nlm.nih.gov/tools/primer-blast⟩. last accessed September 6, 2022.
[29] M. Zuker, Mfold web server for nucleic acid folding and hybridization prediction, Nucleic Acid. Res. 31 (2003) 3406–3415. ⟨http://www.unafold.org⟩. last accessed September 6, 2022.
[30] R. Miranda-Castro, N. de-los-Santos-Álvarez, M.J. Lobo-Castañón, Understanding the factors affecting the analytical performance of sandwich-hybridization genosensors on gold electrodes, Electroanalysis 30 (2018) 1229–1240.
[31] R. Miranda-Castro, R. Sánchez-Salcedo, B. Suarez-Álvarez, N. de-los-Santos-Álvarez, A.J. Miranda-Ordieres, M.J. Lobo-Castañón, M.J, Thioaromatic DNA monolayers for target amplification free electrochemical sensing of environmental pathogenic bacteria, Biosens. Bioelectron. 92 (2017) 162–170.
[32] D. Svec, A. Tichopad, V. Novosadova, M.W. Pfaffl, M. Kubista, How good is a PCR efficiency estimate: Recommendations for precise and robust qPCR efficiency assessments, Biomol. Detect. Quantif. 3 (2015) 9–16.
[33] O. Nordgard, J.T. Kvaløy, R.F. Farmen, R. Heikkila, Error propagation in relative real-time reverse transcription polymerase chain reaction quantification models: the balance between accuracy and precision, Anal. Biochem. 356 (2006) 182–193.
[34] Harmonizome database, ⟨https://maayanlab.cloud/Harmonizome/gene_set/LNCAPCLONEFGC/CCLE+Cell+Line+Gene+Expression+Profiles⟩ (last accessed 6 September 2022).

Raquel Sánchez-Salcedo received her BS in chemistry in 2015 at Universidad Complutense de Madrid. She is now a PhD student in the Electroanalysis research group headed by Prof. M.J. Lobo-Castañón at University of Oviedo and Instituto de Investigación Sanitaria del Principado de Asturias (ISPA). Her research area is the development of electrochemical hybridization-based sensors for cancer biomarkers.

Rebeca Miranda-Castro is Associate Professor at Universidad de Oviedo (Spain). Her research interests focus on the development of electrochemical sensors for clinical diagnosis and food analysis using molecular recognition elements based on nucleic acids (genosensors and aptasensors).

Noemí de-los-Santos-Álvarez received her PhD in Chemistry at University of Oviedo and now is a Full Professor at the same institution. Her initial studies were conducted on electrocatalytic processes and, during her postdoc stage at Cornell University, she switched to the characterization of intermetallic materials for fuel cells. Her current interests are focused on electrochemical genosensors and aptamer selection for cancer biomarkers to be used in in-vitro diagnostics devices.

Daniel Fernández Martínez received the BS in Medicine in 2010 and his PhD in Health Sciences in 2020 from Universidad de Oviedo. He is now Surgeon at Hospital Universitario Central de Asturias and researcher in the Abdominal Surgical Pathology group headed by Dr. L.J. García-Flórez at ISPA. His area of research is the diagnosis and treatment of colorectal cancer.

Luis Joaquin García-Flórez is Surgeon at Hospital Universitario Central de Asturias (HUCA), Associate Professor at the University of Oviedo and leader of the Abdominal Surgical Pathology research group at ISPA. He is head of the Coloproctology section at HUCA, with previous stays at Lahey Clinic Medical Center, UCSF Medical Center, St Mark's Hospital & Academic Institute and Churchill Hospital, Oxford University Hospitals. His areas of expertise are rectal cancer, minimally invasive colorectal surgery, and anal fistula surgery.

María Jesús Lobo-Castañón holds a PhD in Chemistry and leads the Electroanalysis research group at the University of Oviedo in Spain. Since 2017 she is Full Professor in Analytical Chemistry at said University. Her research interests focus on the development of electrochemical sensors for clinical diagnosis and food analysis, using different molecular recognition elements, such as enzymes, DNA and aptamers. She is (co)author of over 130 articles in leading international journals and various book chapters in that field.